# Sliding Mode Position Controller for a Linear Switched Reluctance Actuator

António Espírito Santo,
Maria do Rosário Calado and Carlos Manuel Cabrita
*University of Beira Interior – Electromechanical Engineering Department*
*Portugal*

## 1. Introduction

More than never, the automation of industrial processes has high technical requirements. Today, most of the fabrication processes must operate with an efficient and precise control of different parameters like: velocity, position and torque. Simultaneously, the controller must be immune enough to the outside world perturbations typically found in industry. At the same time, the kind of movement required by today processes is beyond the simple rotational configuration. Linear actuators are making their appearance in the industry, being already a reality and a truly available option that designers and engineers can consider. The traditional conversion method used to transform rotational motion into linear displacement is no more acceptable. In the old days, linear displacement was obtained from a rotational motor shaft, after mechanical conversion by a specific mechanism containing pulleys, worm gears and belts. The presence of these components diminishes the robustness and reliability of the industrial processes.

The ac induction motor has good robustness and low fabrication cost. Over the past decades it has replaced, with great success, the conventional brushed DC motor in servo-type applications. Although this change allowed process reliability improvement, for instance, problems related with the motor brushes are eliminated, the introduction of an electronic power drive increases systems complexity, raising other problems.

The switched reluctance machine (SRM) can be classified as a current-controlled stepping motor of the variable-reluctance type. This technology is one of the most recent options in the field of variable speed actuators. Consumer products, aerospace, and automobile industries are today taking advantage from SRM drives characteristics.

Advances in power electronics and the use of microelectronics and microprocessors allowed the development of different control strategies, such as nonlinear, adaptive, variable structure, and fuzzy, contributing to the popularity that SRM drives actually enjoy.

The SRM is a rugged and reliable actuator, that can be produced at a low cost, presents a simple and robust structure and can operate in a wide speed range, in all four-quadrant, without a considerable reduction of efficiency. These characteristics make it an attractive alternative to permanent-magnet brushless and induction motor drives (Corda, J. et al. (1993)). Its main constructive characteristic is the absence of winding on the rotor of the machine, giving it a potential advantage over conventional machines. Furthermore, the SRM

combines different advantages, such as high power density, low-cost maintenance, the ability to operate even with a phase shorted or opened, and the possibility of direct drive without mechanical transmissions. The power converter design can be very simplified because of the unidirectional stator current. Although most of the control strategies applied to the SRM require the perfect knowledge of rotor position, sensorless operation techniques can also be adopted to control it (Gan, C. et al. (2003)), (Espírito Santo et al. (2005)), (Espírito Santo et al. (2008)).

Nevertheless, the control complexity of these actuators, the high torque ripple presented in output and the acoustic noise produced under normal operation, until recent years, lead to some lack of interest in adopting SRM as a driving technology.

The output power density is increased when the SRM is operated with high saturation levels. Because of this, the SRM flux linkage, inductance, back EMF and phase torque, are highly nonlinear parameters. Furthermore, the SRM cannot operate directly from an AC or DC power supply, requiring a specific electronic controller.

This chapter describes the development of a sliding mode position controller for a linear switched reluctance actuator (LSRA). The main goal of the presented chapter is to control the position of the primary of the actuator. The actuator test bench used is shown in Fig. 1.

The remaining of this chapter describes the energy conversion process of a LSRA. Based on a finite elements analysis, both traction and attraction maps are derived. This information is useful to understand the device working principle and its performance for different excitation and working conditions. The proposed control strategy, based on the sliding mode control technique, and the electronics to drive the LSRA are described. The control strategy was implemented with the TMS320F2812 eZdsp Start Kit, taking advantage of the microprocessor internal peripherals and resources. Finally, the validation of the proposed control strategy is discussed through the presentation of experimental results.
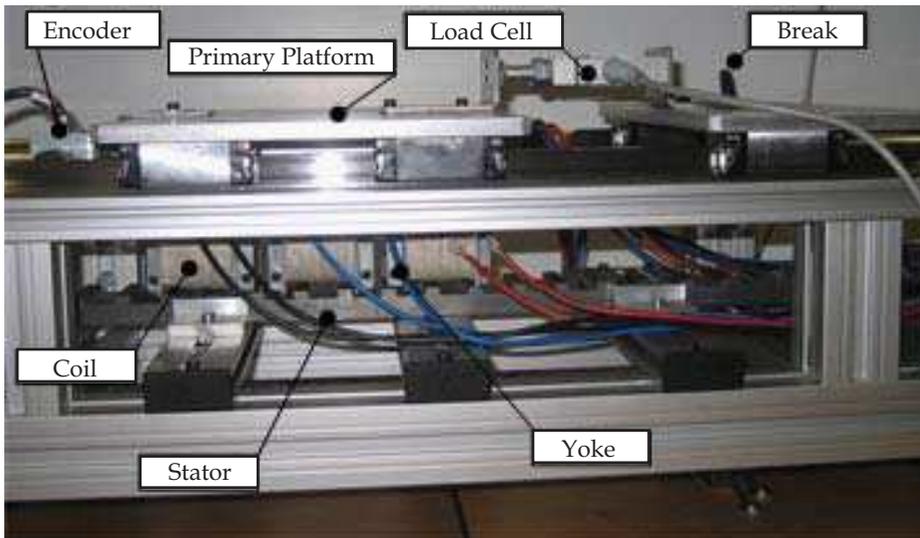


Fig. 1. Actuator experimental test bench.

## 2. The switched reluctance actuator

### 2.1 Introduction to the switched reluctance working principle

The SRM working principle takes advantage from the fact that an electromagnetic system always tries to adopt the geometrical configuration corresponding to the minimum reluctance of the magnetic circuit. In the beginning of the IXX century, scientists from all over the world performed experiments in this field, trying to use the magnetic reluctance principle to produce a continuous movement. The first reference to a SRM appears in a scientific paper published in 1969 by Nasar (Nasar, S. A. (1969)). The first SRM was commercially available in the UK in 1983, and was marketed by TASC Drivers.

In 1838, W.H. Taylor registered two patents of an electromagnetic motor, one in the U.S and the other in the UK (Taylor, W.H. (1840)). Another pioneer in this field was the Scottish engineer Robert Davidson that, in 1838, developed an actuator based in the switched reluctance principle. The actuator constructed by him was used to power an electric locomotive in the Edimburgo-Glasgow railway. Two patents registered in the U.S. by B.D. Bedford and R.G. Hoft, in 1971 and 1972, describe some of the functionalities that can be found in actual SRMs. For instance, the regulation electronics is synchronized with the rotor position. With this information, the motor phases are sequentially energized. Another important step was performed by L. E. Unnewehr and W. H. Koch, from Ford Motor Company Scientific Research Staff Company; they developed an axial SRM controlled by thyristors (Unnewehr, L. E. et al. (1974)). In Europe, others researchers registered several patents, e.g., J. V. Byrne and P. J. Lawrence (Byrne, J.V. (1979)), (Byrne , J.V. et al. (1976)).

A SRM can be used to produce a rotational movement, a linear displacement, or a more complex combination of these movements. The machine primary can be inside of the structure, or outside, and it can be stationary or allowed to move. Typically, the magnetic circuit is energized by independent electric circuits (phases). In turn, the electromagnetic flux from each phase may, or may not, share the same magnetic circuit. Several works related with the SRM can be found in the scientific literature, mainly with respect to the rotational configuration. However, while some of them are related with the linear configuration, papers describing the usage of switched reluctance technology in the production of compound movements are almost non-existent.

Although the SRM is normally used as an actuator, it can also be used as a generator. The phases of a SRM working as motor are energized when the inductance of the phase is increasing, which is to say, when the teeth of the rotor are approaching the poles of the stator. Phases are powered off at the vicinity of the aligned position. The described procedure is inverted when the SRM is operated as a generator. Inductance evolution taking as reference rotor position can be observed in Fig. 2, where aligned and unaligned characteristic positions are identified. It should be observed that the inductance changes not only with rotor position, but also with current. Due to the magnetic saturation effects, at the same position, the inductance value decreases when current value increases.

With the commercial appearance of the SRM, becomes clear the problems related with the acoustic produced noise. The study presented in (Krishnan R. et al. (1998)) allowed to conclude that the acoustic noise has its sources in the vibrations developed by the radial forces acting in the stator. The acoustic noise is amplified when the vibrating frequency matches the mechanical resonant frequency. Acoustic noise can also result from inaccurate mechanical construction or produced by the action of the actuator electronic drive (Chi-Yao Wu et al. (1995)).
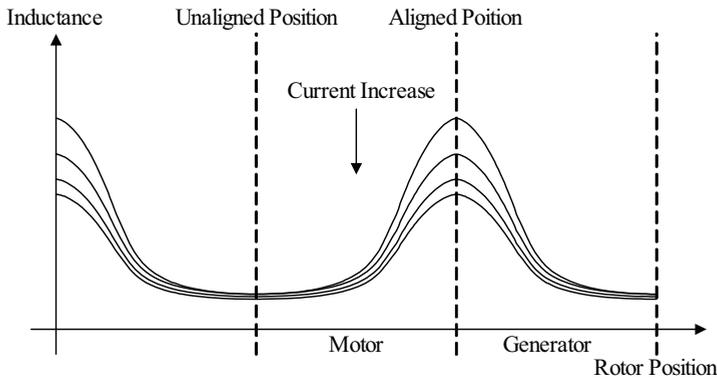
Fig. 2. Inductance variation, taking as reference the rotor position.

A typical geometrical configuration of a SRM can be observed in Fig. 3. This configuration receives the 6/4 designation, because it has six poles in the stator and four teeth in the rotor. Each phase comprises a pair of coils ($A_1$, $A_2$), ($B_2$, $B_2$) and ($C_1$, $C_2$), so there are three phases (A, B, C) in the actuator. Each pair of coils are supported by poles geometrically opposed and are electrically connected in order that the magnetic flux created is additive.

The magnetic force vectors $F_1$ and $F_2$ can be decomposed in two orthogonal components. The axial components $F_{a1}$ and $F_{a2}$ are always equal in magnitude, with opposite directions, and cancel each other out all the time. The transversal components $F_{t1}$ and $F_{t2}$ produce a mechanical torque than changes with current and angular position. If the rotor is withdrawn from the aligned position, in whatever direction (Fig. 3a)), a resistant torque will be created, tending to put the phase at the aligned position again.

At the aligned position (Fig. 3b)) the produced magnetic force doesn't have transversal components and the resulting torque is zero. At this position, the magnetic reluctance has its minimum value; this fulfils the necessary conditions to observe the saturation of the magnetic circuit.

The magnetization curves of a typical SRM are represented in Fig. 4 (Miller, T. J. E, (1993)). The magnetization curves for the intermediate positions are placed between the curves corresponding to those of the aligned and unaligned positions.
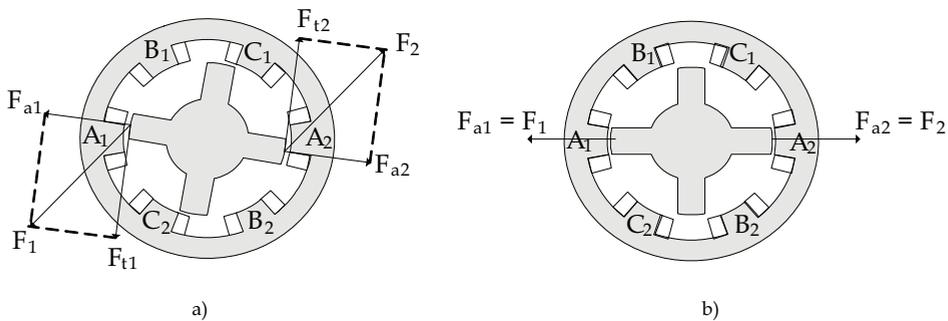


Fig. 3. SRM with phase A energized: a) unaligned position, b) aligned position.
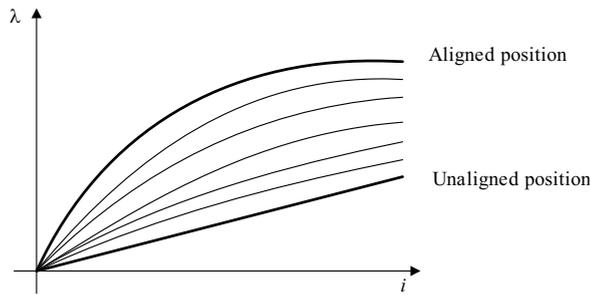
Fig. 4. Typical SRM magnetization curves.

At the aligned and unaligned positions the phase can not produce torque and it is unavailable to start the movement. When a phase is aligned, the others two will be in good position to start the movement in both clockwise and anti-clockwise directions. The previously described situation helps to realize that the SRM can only start by itself, in both directions, if the minimum number of phases is three.

To understand how the switched reluctance actuator works we first need to observe the energy conversion process. The electrical and the mechanical systems are interconnected through the magnetic coupling field. The way how energy flows from the power source to the mechanical load is explained next.

The magnetic reluctance is a measure of the opposition to the magnetic flux crossing a magnetic circuit. If one of the magnetic circuit parts is allowed to move, then, system will try to reconfigure itself to a geometrical shape corresponding to the minimal magnetic reluctance. Fig. 5 illustrates the different stages associated with the energy conversion procedure, when a very fast movement from position $x$ to position $x + dx$ occurs.

Because the movement is fast, it is assumed that the linkage flux does not change. The magnetic field energy $W_{fe}$ at the beginning of the movement is given by the area established in Fig. 5a) as

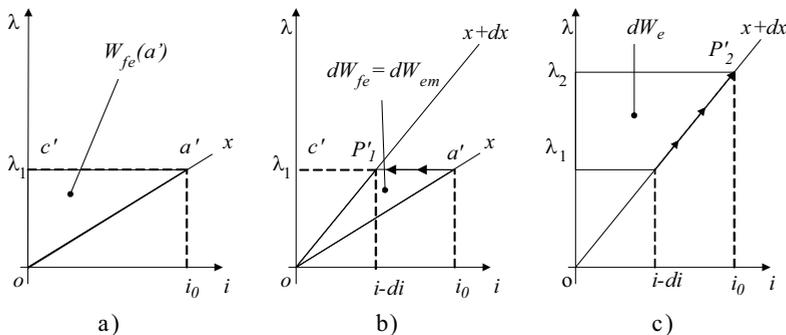$$W_{fe}(a') = \text{area}\{o, a', c', o\}. \tag{1}$$



Fig. 5. Quasi-instantaneous movement from position $x$ to position $x + dx$. a) initial system condition, b) actuator movement, c) power source restoring energy.

When actuator fast displaces from position $x$ to position $x + dx$, represented in Fig. 5b), some of the energy stored in the magnetic coupling field is converted into mechanical energy. This amount of energy is equivalent to the area given by

$$dW_{fe} = \text{area}\{o, a', P_1', o\}. \tag{2}$$

It can be observed that the energy stored at the coupling field decreases. Simultaneously, current also decreases. If voltage from the supply source is constant, the current value will return to its initial value $i_0$, through the path shown in Fig. 5c), restoring the energy taken from the magnetic coupling field during the fast movement.

Because linkage flux is constant throughout the movement, there is no induced voltage and, therefore, the magnetic coupling field does not receive energy from the voltage source.

An electromagnetic device can convert electrical energy into mechanical energy, or vice-versa. The energy responsible for actuator motion, taken from the magnetic coupling field, is expressed by

$$dW_{em} = -dW_{fe} \Rightarrow f_{em} = -\left.\frac{dW_{fe}}{dx}\right|_{\lambda = constant}. \tag{3}$$

The variation of the energy coupling field is equal, but with opposite signal, to the mechanical energy used to move the actuator. The mechanical force $f_{em}$ can be represented by

$$W_{fe} = \frac{1}{2}\frac{\lambda^2}{L} \Rightarrow f_{em} = \frac{\lambda^2}{2L^2}\frac{dL}{dx} = \frac{i^2 dL}{2 dx}. \tag{4}$$

Because $i^2$ is always positive, the force applied to the actuator part allowed to move, in the direction $x$, is also positive as long as the inductance $L$ is increasing in the $x$ direction. So, the mechanical force acts in the same direction, which also increases the magnetic circuit inductance.

The mechanical force can also be calculated by changing the magnetic circuit reluctance with position. If the linkage flux $\lambda$ is constant, then the flux $\varphi$ in the magnetic circuit is also constant and, therefore, the mechanical force is given by

$$W_{fe} = \frac{\Re\varphi^2}{2} \Rightarrow f_{em} = -\frac{\varphi^2}{2}\frac{d\Re}{dx}. \tag{5}$$

The mechanical force $f_{em}$ acts in the direction that puts the actuator in a geometric configuration that corresponds to the path with lower reluctance. The SRM base their work on this basic principle.

We can also define the co-energy as

$$W_{fe}'(i,x) = i\lambda - W_{fe}, \tag{6}$$

depending on current $i$ and position $x$,

$$dW_{fe}'(i,x) = \frac{\partial W_{fe}'(i,x)}{\partial i}di + \frac{\partial W_{fe}'(i,x)}{\partial x}dx. \tag{7}$$

As $i$ and $x$ are independent variables, the linkage flux $\lambda$, inductance $L$ and the mechanical force $f_{em}$ can be obtained from the device co-energy map, applying

$$\begin{cases} \lambda = \dfrac{\partial W_{fe}{'}(i,x)}{\partial i} \Rightarrow L = \dfrac{\lambda}{i} \\ f_{em} = \dfrac{\partial W_{fe}{'}(i,x)}{\partial x} \end{cases} . \tag{8}$$

Thus, as can be seen, if a change in the linkage flux occurs, the system energy will also change. This variation can be promoted by means of a variation in excitation, a mechanical displacement, or both. The coupling field can be understood as an energy reservoir, which receives energy from the input system, in this case the electrical system, and delivers it to the output system, in this case the mechanical system.

The instantaneous torque produced by the actuator is not constant but, instead, it changes according to the current pulses supplied. This problem can be avoided, either by making a proper inspection of the current that flows through the phases, either by increasing the number of phases of the machine.

The operating principle used by the SRM can also be used to build linear actuators. The movement, as in the rotational version, is achieved by the tendency that the system has to reduce the reluctance of its magnetic circuit. In the rotational version, the normal attraction force between the stator and the rotor is counterbalanced by the normal force of the attraction developed by the phase windings which are placed in the diametrically opposite positions, thus contributing to the reduction of the electrodynamic efforts. The linear topology also experiences this situation and because it develops a very high attraction force, designers must have special attention to prevent possible mechanical problems.

The LSRA can have a longitudinal or a transverse configuration (Corda , J. et al. (1993)). In both, the force developed between the primary and the secondary can be vectorially decomposed into attraction and traction force, being the latter one responsible for the displacement. While in the longitudinal configuration the magnetic flux path has a direction parallel to the axis of motion, in the transversal configuration, the magnetic flux has an orientation perpendicular to the axis of movement.

The performance of the two previous configurations can be diminished by the influence of the force of attraction between the primary and secondary. As a consequence, the mechanical robustness of the actuator must be increased. Simultaneously, as already stated, these configurations are more problematic in what concerns the acoustic noise. A symmetric version, with a dual primary, avoids the problems caused by the attraction force. The attraction force developed through a phase, and applied on one side of the secondary, is counterbalanced by the attraction force in the opposite direction, and also applied in the secondary.

A tubular configuration can also introduce significant improvements that minimize some of the problems identified in previous paragraphs. The resultant of the radial forces developed in the tubular actuator will be null. It is therefore possible to use smaller airgaps, because there are no mechanical deformations and thereby maximize the performance of the actuator. In general, the use of ferromagnetic material is maximized. In addition, the construction of the actuator becomes much simpler. The coils can be self-supported and the entire assembly of the structure is greatly simplified. In low-speed applications, eddy

currents can be ignored, since the magnetic flux changes occur more slowly and, therefore, the construction of the magnetic circuit with ferromagnetic laminated material is not mandatory.

## 2.2 LSRA characterization through finite element analysis

Some industrial processes can take advantage from actuators with the ability for doing linear displacements with precision. The switched reluctance driving technology is a valid solution justified by the qualities previously enumerated. The problem to solve will be the development of a new design, not only able to perform linear movements but, simultaneously, that allows the accurate control of its position.

An operational schematic of a LSRA based on the concepts previously introduced can be observed in Fig. 6. This actuator is classified as belonging to the longitudinal class, because the magnetic flux has the same direction as the movement.

The force $F$ developed by each phase can be decomposed in the traction force $F_t$ and the attraction force $F_a$. One of the tasks performed during design procedure is the increase of the traction force and, at the same time, the reduction of the attraction force. While the traction force contributes to the displacement, the attraction force does not produce any useful work and has adverse effects in the mechanical structure, as for example, the changing in the airgap length. Attraction force effects can be minimized through the change of the geometrical configuration of the pole head.
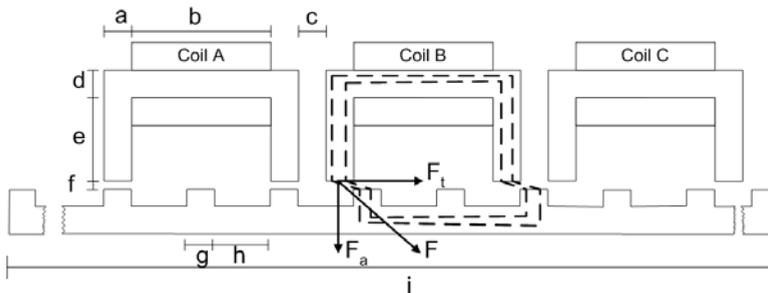


Fig. 6. LSRA physical dimensions.

The physical dimensions of the actuator are listed in Table 1.

| | |
|---|---|
| Yoke pole width (a) | 10 |
| Coil length (b) | 50 |
| Space between phases (c) | 10 |
| Yoke thickness (d) | 10 |
| Yoke pole depth (e) | 30 |
| Airgap length (f) | 0.66 |
| Stator pole width (g) | 10 |
| Stator slot width (h) | 20 |
| LSRA length (i) | 2000 |
| LSRA stack width | 50 |

Table 1. LSRA physical dimensions [mm]

Finite elements tools allowed to study the complexity of this technology (Ohdachi, Y., (1997)), (Brisset, S. et al. (1998)). But there is still missing a standard method to assist the design of this class of actuators, although several proposals have been published until now (Krishnan, R. et al. (1998)), (Anwar , M. N. et al. (2001)).

A Finite Elements Model (FEM) of a single-phase LSRA was constructed using FLUX2D. FEM construction starts with geometric model definition, where each specific region is defined through points and lines. The FEM constructed for the analysis of a single-phase actuator can be observed in Fig. 7.



a)



b)
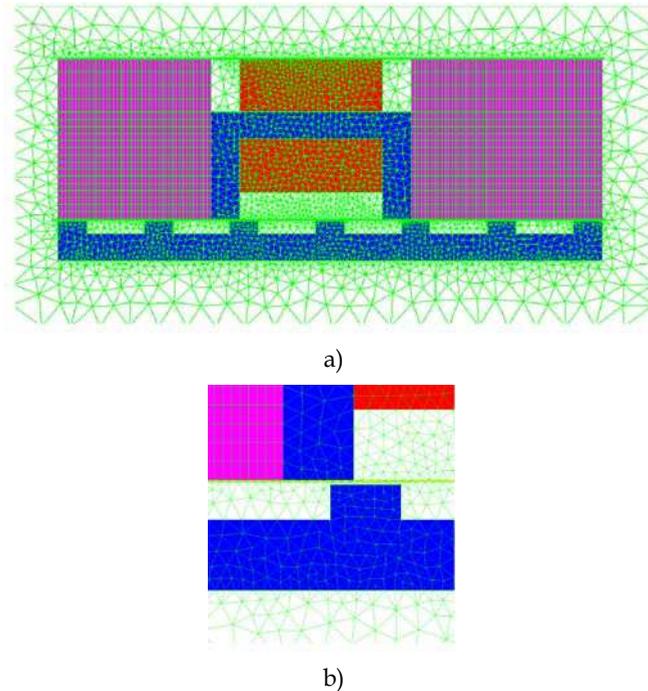
Fig. 7. Finite Elements Model of a single-phase actuator:  a) global view and b) polar region detail.

One of the used finite elements software FLUX2D features is the translation displacement possibility, allowing the longitudinal displacement of one, or a group, of regions, without the need of redefining the geometry of the model and respective finite element mesh. Two regions (in magenta) are defined between the set of regions that must be displaced in the longitudinal direction throughout the static simulations. These regions are the actuator primary (in blue), the phase coil that carries current in the positive direction (inner region) and negative direction (outer region) (both in red), and respective surrounding air (in white). Translation function demands also the definition of two narrow airgap regions (in yellow), located in both side of the translations regions, and used for the displacement of the regions defined between them.

All regions use triangular elements in the finite elements mesh creation. The exceptions are the two displacement regions that use quadrangular elements. Mesh creation must also

observe that only a single layer of elements can be established in the translations air-gap regions.

Primary and secondary regions are associated to materials with ST-37 steel magnetic characteristics. All other regions inherit the vacuum magnetic characteristics. Inside the coil regions, a current source is defined with a positive value for the region that carries the current in the positive direction and an identical negative value for the region that carries the current in the negative direction. Dirichlet conditions are formulated in the model boundary, imposing a null flux across it.

Several simulations were performed for a set of primary positions and currents. Obtained phase traction force $F_t$ and attraction force $F_a$ maps are presented in Fig. 8.

As can be observed, when actuator poles are aligned (position $x = 0$ mm) with the secondary teeth the traction force is zero. This same situation occurs also at non-aligned positions (position $x = 15$ mm and $x = -15$ mm). From the analysis of the attraction force map is possible to conclude that maximum attraction force is obtained at the aligned position (position $x = 0$ mm).
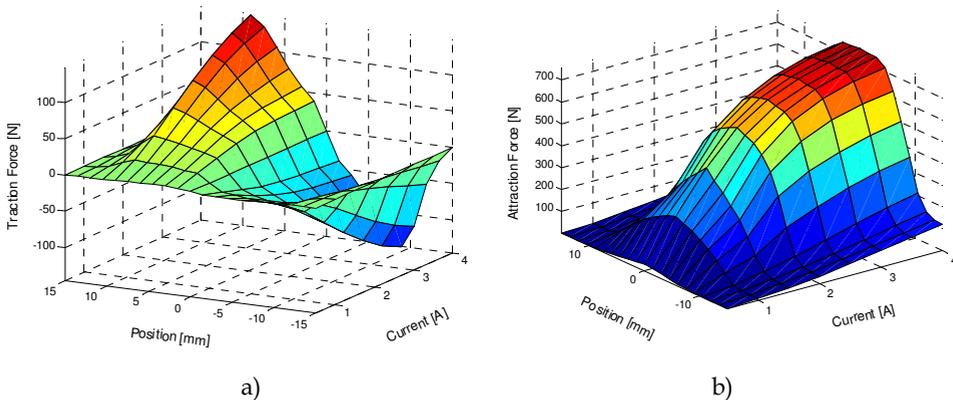


a)                                                                b)

Fig. 8. LSRA force maps as a function of position and current: a) traction force and b) attraction force.

### 2.3 LSRA step-by-step operation control

The configuration of the LSRA with independent phases allows to increase the robustness of the actuator and improves its performance, because more than one phase can operate simultaneously, without any kind of disturbance among them. The number of phases of the actuator can also be easily changed.

The sequential energization of the actuator phases is a simple control methodology, which can be implemented without requiring large computational resources. Typically, turn-on and turn-off positions are established. As demonstrated by the FEM simulations, the traction force depends on position and current. For each phase, the attraction force developed at the aligned and unaligned positions is always zero. As a consequence, for these positions, the phase can't contribute to displace the actuator. Between these two positions, the traction force direction depends of the relative positions between phase poles and the nearest stator teeth.
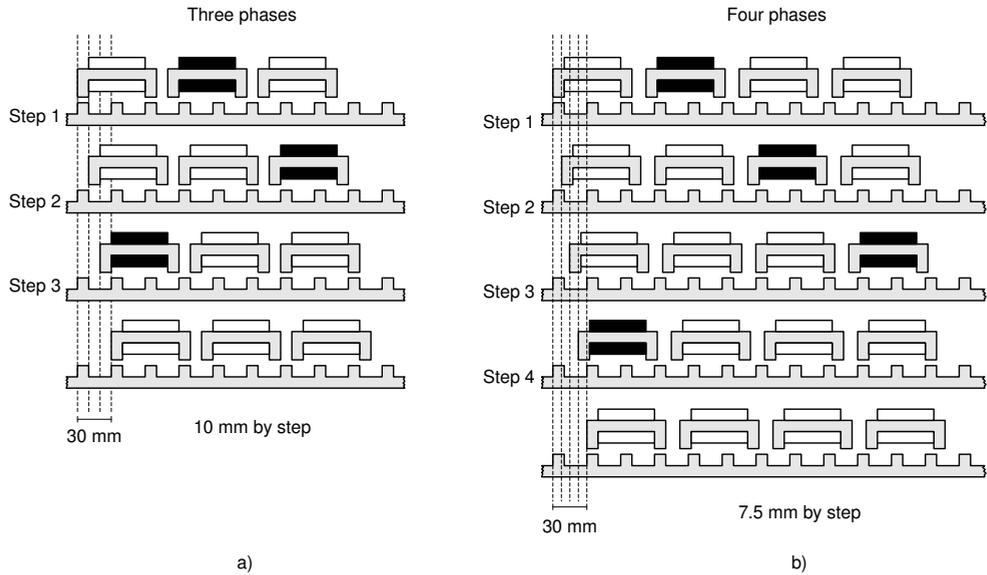
Fig. 9. LSRA step-by-step motion: a) three phases configuration; b) four phases configuration.
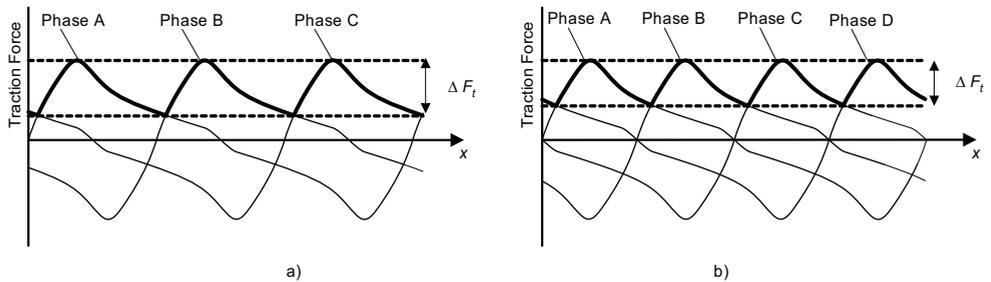


Fig. 10. LSRA step-by-step motion: a) three phases configuration; b) four phases configuration.

Considering phase A at the aligned position as the displacement reference ($x$ = 0 mm), the motion can be started in both directions, depending on the energization of the others two phases. If phase B is energized, the actuator will be moved to the right. The movement to the left can be achieved through the energization of phase C.

Operation of the actuator in three phase configuration is represented in Fig. 9a). With this configuration the actuator can perform displacements with 10 mm of resolution. In Fig. 10a) is illustrated a schematic representation of the total traction force developed by all the three phases, considering that they are energized with a constant value of current. It can be observed that the traction force isn't constant and changes with position. In the example, the actuator performs a displacement of 30 mm to the right. During this movement all phases are energized in B-C-A order.

Actuator performance can be improved if the number of phases is increased. A 30 mm displacement is represented in Fig 9b), for an actuator with four phases energized in

B-C-D-A order. It can be observed that the resolution of the displacement was increased to 7.5 mm. At the same time, the total traction force ripple was also decreased, see Fig. 10b). The major drawback observed is that the size and the height of the actuator increase.

## 3. Sliding mode position controller

The sliding mode technique was used by others to control the behaviour of SRM. Through it, problems as the acoustic noise, binary flicker, or velocity control were solved with success or, at least, machine performance was improved.

A direct torque control algorithm for a SRM using sliding mode control is reported in (Sahoo, S.K. et al. (2005)). A control strategy for an energy recovery chopper in a capacitor-dump is proposed in (Bolognani, S. et al. (1991)). A flux-linkage controller, using the sliding mode technique, with integral compensation, is proposed in (Wanfeng Shang et al. (2009)) for torque ripple minimization. A sliding mode controller is used in (Pan, J. et al. (2005)) to control the position of a two-dimensional (2D) switched reluctance planar motor.

An approximate sliding mode input power controller and another feedforward sliding mode speed controller are combined with space voltage vector modulation in (Tzu-Shien et al. (1997)) to implement a robust speed control. Another robust speed controlled drive system using sliding mode control strategy is presented in (John, G. et al. (1993)).

A sliding-mode observer is proposed in (Zhan, Y.J. et al. (1999)) for indirect position sensing. A sliding mode binary observer is also used in (Yang, I.-W. et al. (2000)) to estimate the rotor speed and position. Current and voltage are used by a sliding mode observer described in (Islam, M.S. et al. (2000)) to estimate the position and the speed to minimize the torque-ripple. The conduction angles are controlled in (McCann, R.A. et al. (2001)) by a sliding mode observer that estimates the rotor position and the velocity.

A sliding mode controller is used in (Xulong Zhang et al. (2010)) in order to reduce cost, simplify the system structure and increase the reliability of a switched reluctance generator.

The LSRA electromagnetic model to n = {1,2,3} phases is described by (9), where $R_n$ is the phase coil resistance, $v_n$ the supplied voltage and $i_n$ the phase current. Mathematical expression (10) describes actuator mechanical behaviour, where $a$ is the device acceleration and $M$ the mass. Actuator non-linearity is taken into account because both inductance $L(i,x)$ and traction force $F(i,x)$ change not only with position $x$, but also with current $i$.

$$0 = R_n i_n(t) + \frac{dL(i_n,x)i_n(t)}{dt} - v_n = \frac{di_n}{dt}\left[L(i_n,x) + i_n(t)\frac{\delta L(i_n,x)}{\delta i}\right] + \frac{dx}{dt}\left[\frac{\delta L(i_n,x)}{\delta x}\right]R_n i_n(t) - v_n \quad (9)$$

$$a = \frac{F(x,t)}{M} \quad (10)$$

The state space is defined as:

$$\begin{cases} \dfrac{dx}{dt} = y \\[2mm] \dfrac{dy}{dt} = \dfrac{F}{M} \\[2mm] \dfrac{di_n}{dt} = \dfrac{y\beta_n + R_n i_n - v_n}{\alpha_n} \end{cases} \quad (11)$$

where $\alpha_n$ and $\beta_n$ stands for:

$$\begin{cases} \alpha_n = L(i_n,x) + i_n \dfrac{\delta L(i_n,x)}{\delta i} \\[3mm] \quad\;\; \beta_n = i_n \dfrac{\delta L(i_n,x)}{\delta x} \end{cases} \tag{12}$$

The control strategy previously presented allows to reach discrete positions. Intermediate positions aren't reachable. The concept of variable structure is introduce next, and applied to the LSRA to improve the displacement capacities the actuator. The Variable Structure System (VSS) as defined below

$$\dot{X} = A(X,t) + B(X,t)u \,, \tag{13}$$

belongs to a particular case of automatic control systems. Intentional commutation is introduced between two different control actions, in one or more channels of control inputs. The possible type of motion of a VSS in the state space is manifested by the appearance of the sliding mode regime. This kind of control was successively applied to the rotational switching reluctance motors as described previously. To achieve sliding motion regime, a switching surface is defined by $s(X,t) = 0$, the control structure $u(X,t)$ stated in (14) changes from one structure to another. When $s(X,t) > 0$ the variable structure control is changed in order to decrease $s(X,t)$. The same kind of action is taken when $s(X,t) < 0$. The control main goal is to keep the system state space sliding in the surface $s(X,t) = 0$. During this sliding motion, the system behaves like a reduced-order system, being insensitive to disturbances and parameters changes. The control structure can be expressed by:

$$u(X,t) = \begin{cases} u^+(X,t) & \Leftarrow \quad s(X) > 0 \\ u^-(X,t) & \Leftarrow \quad s(X) < 0 \end{cases}. \tag{14}$$

The previously explained concept is used to develop the LSRA position controller. At a specific moment, it is assumed that traction force can be developed in both directions with proper choice of actuator phase. After turning off, an actuator phase still has the ability to produce traction force. This situation occurs because current phase do not goes down instantaneously, but diminishes by the free wheel diodes path, with a time constant that depends on phase inductance and resistance. This behaviour is responsible for the introduction of a delay in controller response, contributing to increase the oscillations (chattering) around the sliding surface.

The movement of the actuator can be expressed as a VSS with two possible control actions. Considering that the primary of the actuator has the M mass. A control action produces a traction force in the left direction $F_l$, while the other control action produces a traction force in the right direction $F_r$. Under this control action the actuator will have the horizontal displacement $x$, at velocity $y$, given by

$$\begin{cases} \dot{x} = y \\[2mm] \dot{y} = \dfrac{u}{M} \end{cases}. \tag{15}$$

The control law $u(t)$ is established as

$$u(t) = \begin{cases} F_r & \Leftarrow & s(e,\dot{e}) > 0 \\ F_l & \Leftarrow & s(e,\dot{e}) < 0 \end{cases},$$  (16)

The VSS model has the following formulation

$$\begin{cases} \dot{x} = y \\ \dot{y} = k\dfrac{F_\gamma}{M} + (1-k)\dfrac{F_l}{M} \end{cases},$$  (17)

with $k \in \{0,1\}$.
The system will be defined by

$$\dot{x} = f(x) + g(x)k ,$$  (18)

with

$$f(x) = \begin{bmatrix} y \\ F_l/M \end{bmatrix} \quad and \quad g(x) = \begin{bmatrix} 0 \\ (F_r - F_l)/M \end{bmatrix}.$$  (19)

The commutation function $s(e,\dot{e})$ depends on the position error $e$ and the derivative of the position error $\dot{e}$, and is defined by

$$s(e,\dot{e}) = me + \dot{e} ,$$  (20)

where $m$ is a positive constant, experimentally obtained.
The controller selects from the lookup Table 2 which phase will provide the desired control action, in order to maintain $s(e,\dot{e}) = 0$. The position reference ($x = 0$) is taken as the aligned position for phase A.

| Traction Force | [0,10[ | [10,20[ | [20,30[ |
|---|---|---|---|
| Left direction ($F_l$) | Phase A | Phase B | Phase C |
| Right direction ($F_r$) | Phase B | Phase C | Phase A |

Table 2. Relative actuator position [mm]

## 4. Regulation and command electronic driver

For the actuator could be able to perform the predefined task with the required performance, a power converter must be designed for driving it and to apply the proposed control strategy. The half-bridge configuration has the required versatility to permit the usually adopted operation modes in applications with SRM: single-pulse, soft-chopping and hard-chopping. An example of a functional structure of the controller for one phase can be seen in Fig. 11.
The developed power converter has three main blocks (Fig. 12), which are (1) the Distribution Unit, responsible to make the interface with the microprocessor using proper electronics and to manage the operation of the other two blocks, (2) the Regulation Units receive orders concerning the states that must be imposed to the power switches; making use of the reference

signal available from the microprocessor, have the ability to control the shape of the current that flows in each coil of the actuator phases, (3) the Power Units, which, receiving orders from the state of the power switches, can properly feed the phase coils.
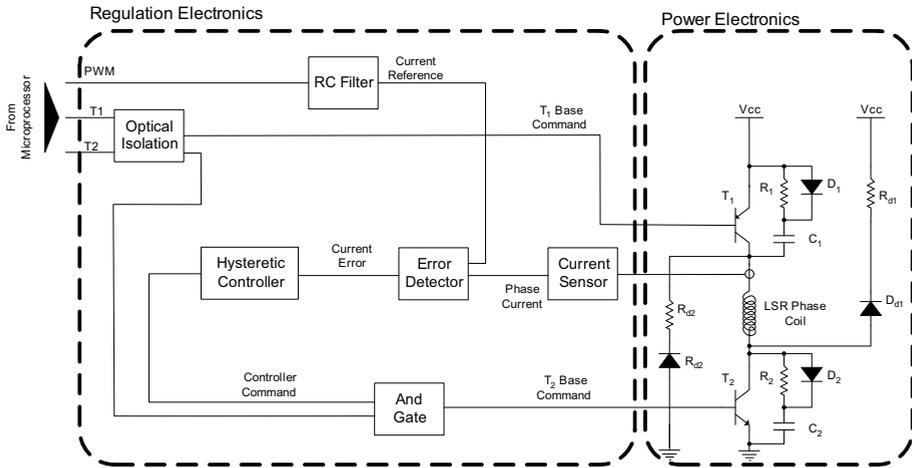
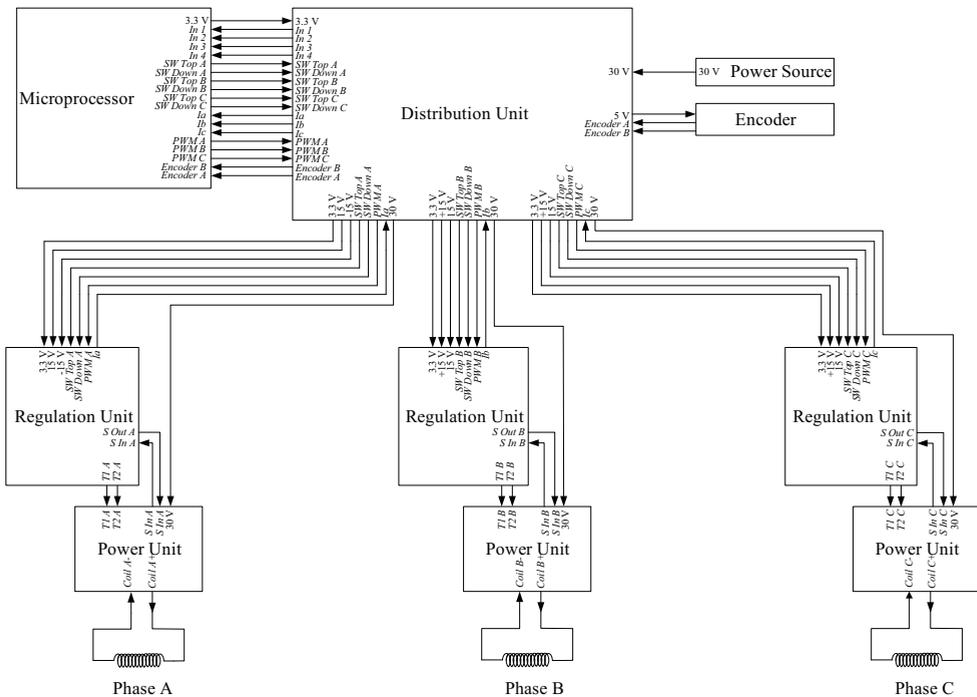Fig. 11. Power converter general topology for one phase.

Fig. 12. Global visualization of the actuator driver.

All the information is centralized in the Distribution Unit, which shares that information with the processor, and for each phase is possible to know the required PWM (Pulse-Width Modulation) signal used to generate the controller current reference, the state of the switch $T_1$, the state of the switch $T_2$, and the signal corresponding to the current in the coil of the actuator phase. Beyond these knowledge, the Distribution Unit receives from the encoder two lines with pulse sequences (Encoder A and Encoder B), which are sent to the microprocessor, allowing the determination of both the position and the direction of the displacement.

The analog signal, reference of the current controller, is generated by a DAC (Digital-to-Analog Converter), by using a PWM. The signal, after being filtered by a low-pass filter is returned as a signal depending on the band width of the PWM. The DAC resolution is stated by the length of the counter used to generate the PWM signal.

The resolution $R_{bit}$, in number of bits, can be calculated as

$$R_{bit} = Log_2(R) = Log_2\left(\frac{N_{max}}{C}\right) = \frac{\ln\left(\frac{N_{max}}{C}\right)}{\ln(2)}, \tag{21}$$

with $R = N_{max} / C$, $N_{max}$ the maximum number of counts and $C$ the minimum change of duty-cycle. As an example, with a maximum count of 512 and 2 the minimum change of the duty-cycle, the obtained resolution is of 256 different levels for the analog output. The corresponding resolution in bits is

$$R_{bit} = \log_2(256) = 8\,\text{bits} \tag{22}$$

The required frequency of the PWM is established by the rate of change stated by the DAC, as each change in the duty-cycle corresponds to a sample of the DAC. The frequency of the counter $f_c$ depends on the frequency $f_{PWM}$, stated for the PWM signal, and on its resolution $R_{bit}$. So, it can be written that

$$f_c = 2^{R_{bit}} f_{PWM} \tag{23}$$

Thus, in order to obtain an 8 bits equivalent DAC, able to generate signals with 8 kHz frequency samples, the PWM signal must have a similar frequency. Using the equation (23), the counter must receive a clock input with a frequency of 2.048 MHz. The cut-off frequency of the low-pass filter must be defined quite below the frequency of the PWM signal, so that the noise generated by the signal commutation can be canceled. Nevertheless, it can't be so small that restricts the rate of change of the DAC output by imposing a high time constant.

The acquisition of the current flowing in the phase coil is achieved by using a Hall effect sensor with dynamic characteristic that enables it to follow the variations in the signal to be acquired.

The comparator is used to compare the voltages applied to its two input ports and return a value depending on the sign of the difference between those values (Franco, S. (2001)), (Williams, J. (1990)). This device can be faced as an analog to digital converter of one single bit.

When the amplifier feedback signal is positive, it can be said that it is in regenerative operation mode. In this situation, the circuit acts in order to amplify the effect of any

disturbance. The amplifier output can then adopt one of two states: high or low levels. The obtained hysteresis characteristic can be used in implementing the on-off type control.
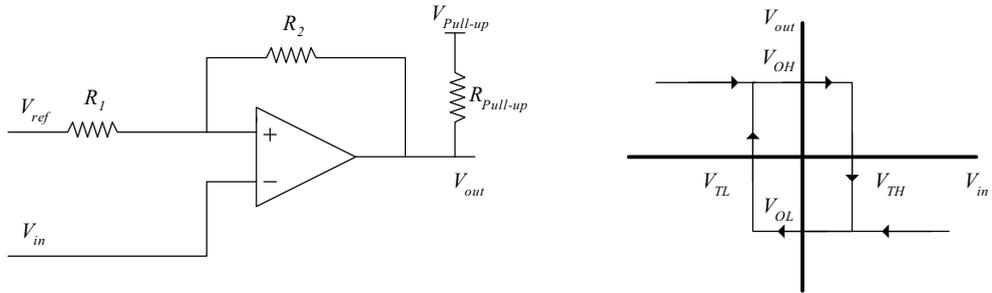


Fig. 13. Scheme of hysteresis control circuit in inverting assembly

In the electrical scheme of Fig 13, the signal $V_{in}$ is applied to the inverting input and the resistance $R_2$ is much higher than the resistance $R_1$. In the special case of having infinite resistance $R_2$ there will be no hysteresis, and the circuit switch on with the reference of voltage $V_{ref}$.

$$V_{TL} = \left(R_2 V_{\text{Ref}} + R_1 V_{OL}\right)/\left(R_1 + R_2\right)$$
$$V_{TH} = \left(R_2 V_{\text{Ref}} + R_1 V_{OH}\right)/\left(R_1 + R_2\right) \qquad (24)$$
$$\text{Hysteresis gap} = V_{TH} - V_{TL} = R_1\left(V_{OH} - V_{OL}\right)\left(R_1 + R_2\right)$$

All the electronic chain used to control the current flowing in the phase coil is represented in Fig. 14, being the way how it is integrated in the power converter operation described as follows.
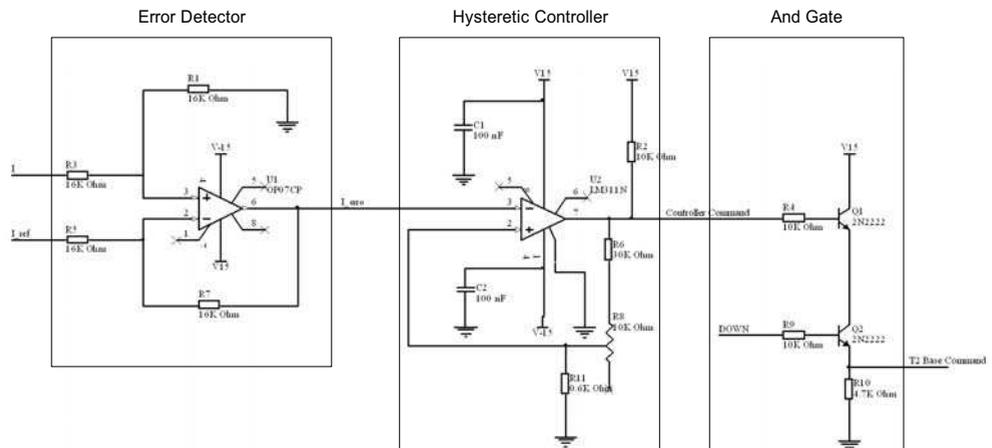


Fig. 14. Circuit used to control the current flowing in the actuator phase coil.

Once the current *I* flowing in the actuator phase coil is acquired and conditioned, the value of the reference current *I_ref* is subtracted; the resulting value from that operation, *I_error*, is sent to the histeresis controller, with the histeresis range set by the potentiometer $R_8$. The resistance $R_2$ is used to make the pull-up of the control output signal. The output signal is available to the following electronic structure, which operates as an AND logical gate. If the current flowing through the base-emitter diode is enough high to saturate it, the collector voltage can be less than 1 volt, which is considered as a logic TTL zero. The result from that logical operation is the basis to establish the control of the power switches of the half-bridge power converter $T_2$. Thus, the switch is only activated if there are simultaneous orders from the microprocessor and from the histeresis controller.

With the current controller it can be established a current profile. In Fig. 15 is possible to observe how voltage at the phase coil is switched for different current profiles.



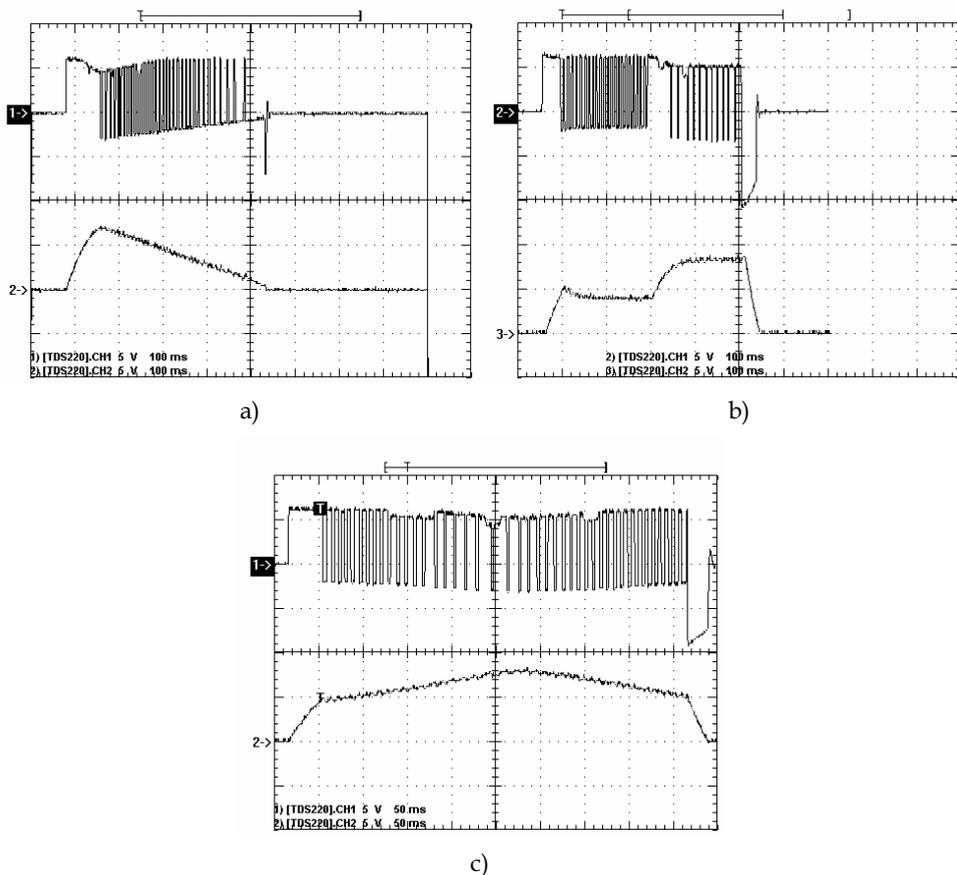a)                                                                    b)



c)

Fig. 15. Actuator hardware current controller operation: voltage (ch. 1) e current (ch. 2): a) current decreases linearly, b) two different current stages, c) increasing and decreasing the current linearly.

## 5. Development of the controller firmware

To verify the applicability of the here proposed control methodology, an experimental setup was constructed based on the TMS320F2812 eZdsp Start Kit. Event Manager EVA is used to generate the PWM signals from where the Current Reference signals are obtained. Each current phase signal is acquired by the on-chip ADC and saved in a buffer memory. At this moment current phase information is not used by the controller.

Actuator position is feedback to the TMS320F2812 QEP Unit by the incremental encoder. From the Quadrature Encoder Pulse (QEP) unit data, actuator velocity and position are derived. The sliding mode controller establishes the switching strategy, used to turn-on and turn-off the LSRA phases. Using Microcontroller GPIO, each phase signal lines $T_1$ and $T_2$ are properly switched. Data lines shared between the eZdsp and the LSRA regulation electronics are represented in Fig. 16a).
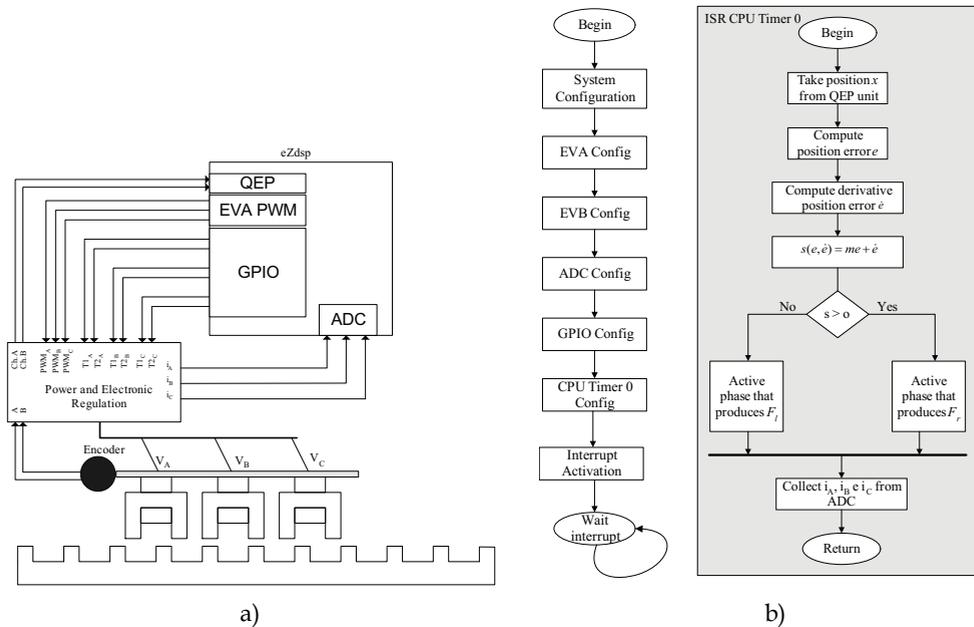


Fig. 16. a) eZdsp interface with LSRA electronic regulation and b) TMS320F2812 code flow.

Developed code to the TMS320F2812 implements the control methodology previously described. The most important software blocks are represented at Fig. 16b). Software begins with the configuration of each peripheral and before enter in a wait state activates the CPU Timer 0 interrupt. This interrupt possess an ISR that based in QEP information determines the actuator position and, based on it, the corresponding position error and derivative position error. For each CPU Timer 0 interrupt a service routine is executed. The information needed to realize the control procedure is obtained. Based on it, the control action is derived and applied to the proper phase, as specified in the lookup table. Status system information (position and phase current) is saved in memory. After the operation action, the functionalities of Code Composer Studio are used to collect the results from the microprocessor memory and saved it on file for posterior analysis.

## 6. Results and discussion

The results returned by the application of the sliding mode control methodology to the LSRA are presented next. The primary of the actuator always start from the initial position ($x = 0$) with the poles of the phase A aligned with the stator teeth. The information on the displacement that the primary of the actuator must perform is provided to the sliding mode controller. Position evolution of primary of the actuator is presented in Fig. 17 for different required final positions.

For one of the previous displacements (25 mm) the phase portrait is presented in Fig. 18.
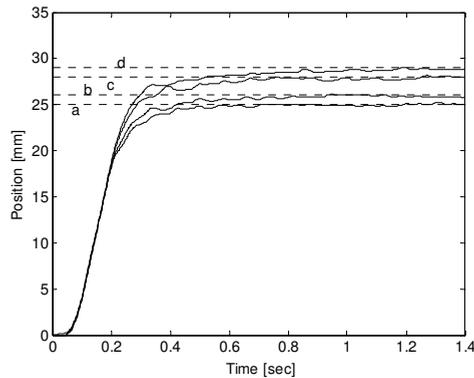


Fig. 17. Actuator position for small displacements: a) 25 [mm], d) 26 [mm], c) 28 [mm], d) 29 [mm].
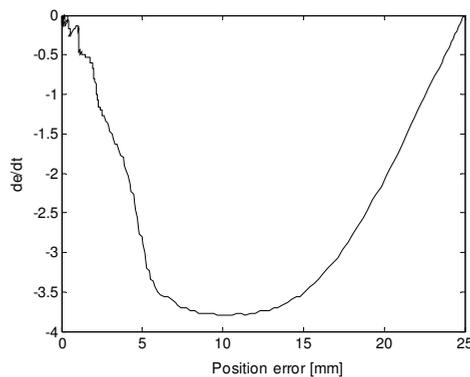


Fig. 18. Phase portrait for a 25 [mm] displacement.

## 7. Conclusion

The finite elements analysis allowed to understand the working principle of a three phase Linear Switched Reluctance Actuator developed for robotics applications. Using this tool, traction and attraction map were obtained. This information allows to characterize the actuator behaviour. Based on the obtained results a prototype was constructed with

correspondent power and regulation electronics. The establishment of proper position control for a high performance device was achieved through a proposed strategy based on sliding mode control. That task was performed by implementing the developed methodology on a TMS320F2812 eZdsp Start Kit, taking advantage from their built-in peripherals. Experimental results allowed to conclude that actuator can realize displacements with 1 [mm] resolution.

## 8. References

Anwar , M. N.; Husain I.; Radun A. V., (2001). "A Comprehensive Design Methodology for Switched Reluctance Machines," *IEEE Transactions on Industry Applications*, Vol. 37, No. 6, pp. 1684-1692, November/December 2001.

Bolognani, S.; Ognibeni, E.; Zigliotto, M.; (1991). "Sliding mode control of the energy recovery chopper in a C-dump switched reluctance motor drive," in *Proceedings of Applied Power Electronics Conference and Exposition*, 1991. APEC '91. Conference Proceedings, 1991., Sixth Annual , vol., no., pp.188-194, 10-15 Mar.

Brisset, S.; Brochet, P., (1998). "Optimization of Switched Reluctance Motors using Deterministic Methods with Static And Dynamic Finite Element Simulations," *IEEE Transactions on Magnetics*, Vol. 34, No. 5, pp. 2853-2856, September.

Byrne , J.V.; Lacy, J.C., (1976). United States Patent No. 3,956, 678, May 11.

Byrne, J.V., (1979). German Patent No. DT 20 30789 B2, 23 June.

Chi-Yao Wu, Pollock, C., (1995). "Analysis and Reduction of Vibration and Acoustic Noise in the Switched Reluctance Drive, (1995)." *IEEE Transactions on Industry Applications*, Vol. 31, No. 1, pp. 91-98, January/ February.

Corda , J.; Skopljak , E., (1993) "Linear Switched Reluctance Actuator," in *Proceedings of the Sixth International Conference on Electrical Machines and Drives*, pp.535-539, September.

Corda, J. ; Skopljak, E, (1993). "Linear switched reluctance actuator," in *Proceedings of the Sixth International Conference on Electrical Machines and Drives*.

Espírito Santo, A.; Calado M. R. A. ; Cabrita, C. M. P., (2005). "Variable Reluctance Linear Actuator Dynamics Analysis Based on Co-energy Maps for Control Optimization," in *Proceedings of Linear Drives for Industry Application*.

Espírito Santo, A.; Calado M. R. A. ; Cabrita, C. M. P., (2008). "Analysis and Position Control of a Linear Switched Reluctance Actuator Based on Sliding Mode Control," in *Proceedings of the 13th International Conference on Power Electronics and Motion Control*, September.

Franco, S., (2001). *Design With Operational Amplifiers and Analog Integrated Circuits*, McGraw-Hill.

Gan, C. ; Cheung, N. C. ; Qiu, L., (2003). "Position Control of Linear Switched Reluctance," *IEEE Transactions on Industry Applications*, vol. 39, no. 5, September/October.

Hung, J. Y. ; Gao, W.; Hung, C, (1993). "Variable Structure Control: A Survey," *IEEE Transactions on Industrial Electronics*, vol. 40, no. 1, February.

Islam, M.S.; Husain, J., (2000). "Torque-ripple minimization with indirect position and speed sensing for switched reluctance motors," *IEEE Transactions on Industrial Electronics*, vol.47, no.5, pp.1126-1133, Oct.

John, G.; Eastham, A.R., (1993). "Robust speed control of a switched reluctance drive," in *Proceedings of Electrical and Computer Engineering*, 1993. Canadian Conference on , vol., no., pp.317-320 vol.1, 14-17 Sep.

Krishnan R.; Vijayraghavan, P., (1998). "State of the Art: Acoustic Noise in Switched Reluctance Motor Drives," in *Proceedings of the 24th Annual Conference of the Industrial Electronics Society* – IECON98, pp. 929-934.

Krishnan, R., Arumugam, R., Lindsay J. F., (1998). "Design Procedure for Switched-Reluctance Motors," *IEEE Transactions on Industry Applications*. Vol. 24, No. 3, pp. 456-461, May/June.

McCann, R.A.; Islam, M.S.; Husain, I., (2001). "Application of a sliding-mode observer for position and speed estimation in switched reluctance motor drives," *IEEE Transactions on Industry Applications*, vol.37, no.1, pp.51-58, Jan/Feb.

Miller, T. J. E, (1993). *Switched Reluctance Motors and their Control*, Magna Physics Publishing Oxford Science Publications.

Nasar, S. A., (1969). "DC Structures Reluctance Motor," *IEE Proceedings* Vol. 116, No. 1048-9.

Ohdachi, Y., (1997) "Optimum Design of Switched Reluctance Motors Using Dynamic Finite Element Analysis," *IEEE Transactions on Magnetics*, Vol. 33, No. 2, pp. 2033-2036, March.

Pan, J.; Cheung, N.C.; Jinming Yang, (2005). "High-precision position control of a novel planar switched reluctance motor," *IEEE Transactions on Industrial Electronics*, vol.52, no.6, pp. 1644- 1652, Dec.

Sahoo, S.K.; Panda, S.K.; Xu, J.X., (2005). "Direct Torque Controller for Switched Reluctance Motor Drive using Sliding Mode Control," in *Proceedings of Power Electronics and Drives Systems*, 2005. PEDS 2005. International Conference on , vol.2, no., pp. 1129-1134, 28-01 Nov.

Taylor, W.H., (1840). "Obtaining Motive Power," Patent No.8255, England, 2nd May 1840.

Tzu-Shien Chuang; Pollock, C., (1997). "Robust speed control of a switched reluctance vector drive using variable structure approach," *IEEE Transactions on Industrial Electronics*, vol.44, no.6, pp.800-808, Dec.

Unnewehr, L. E.; W. H. Koch, (1974)."An Axial Air-Gap Reluctance Motor For Variable Speed Applications," *IEEE Transactions on Power Apparatus and Systems*, Volume: PAS-93, Issue: 1, pp. pp. 367-376, January.

Wanfeng Shang; Shengdun Zhao; Yajing Shen; Ziming Qi, (2009). "A Sliding Mode Flux-Linkage Controller With Integral Compensation for Switched Reluctance Motor," *IEEE Transactions on Magnetics*, vol.45, no.9, pp.3322-3328, Sept.

Williams, J. (1990). "High-speed Comparator Techniques," *Application Note AN-13*, Linear Technology.

Xulong Zhang; Guojun Tan; Songyan Kuai; Qihu Wang, (2010). "Position Sensorless Control of Switched Reluctance Generator for Wind Energy Conversion," in *Proceedings of Power and Energy Engineering Conference* (APPEEC), 2010 Asia-Pacific , vol., no., pp.1-5, 28-31 March.

Yang, I.-W.; Kim, Y.-S., (2000). "Rotor speed and position sensorless control of a switched reluctance motor using the binary observer," in *IEE Proceedings Electric Power Applications*, vol.147, no.3, pp.220-226, May.

Zhan, Y.J.; Chan, C.C.; Chau, K.T., (1999). "A novel sliding-mode observer for indirect position sensing of switched reluctance motor drives," *IEEE Transactions on Industrial Electronics*, vol.46, no.2, pp.390-397, Apr.
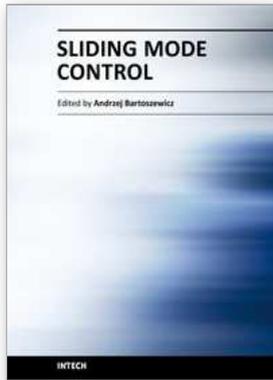
**Sliding Mode Control**

Edited by Prof. Andrzej Bartoszewicz

The main objective of this monograph is to present a broad range of well worked out, recent application studies as well as theoretical contributions in the field of sliding mode control system analysis and design. The contributions presented here include new theoretical developments as well as successful applications of variable structure controllers primarily in the field of power electronics, electric drives and motion steering systems. They enrich the current state of the art, and motivate and encourage new ideas and solutions in the sliding mode control area.

**How to reference**

In order to correctly reference this scholarly work, feel free to copy and paste the following:

# INTECH
open science | open minds